J. Fluid Mech. (1986), *vol.* 163, *pp.* 129–140
Printed in Great Britain

Unsteady boundary layers with an intelligent numerical scheme

By TUNCER CEBECI
Douglas Aircraft Company, Long Beach, CA

(Received 10 October 1984 and in revised form 14 August 1985)

A numerical method has been developed to represent unsteady boundary layers with large flow reversal. It makes use of the characteristic box scheme which examines the finite-difference grid in relation to the magnitude and direction of local velocity and reaches and implements a decision to ensure that the Courant, Friedricks & Lewey stability criterion is not violated. The method has been applied to the problem of an impulsively started circular cylinder and the results, though generally consistent with those of van Dommelen & Shen obtained with a Lagrangian method, show some differences. The time step is identified as very important and, with the present intelligent numerical scheme, the results were readily extended to times far beyond those previously achieved with Eulerian methods. Extrapolation of the results suggests that the much-discussed singularity for this unsteady flow is the same as that of the corresponding steady flow.

1. Introduction

Until recent work by van Dommelen & Shen (1981, 1982), controversy existed with regard to the possibility that a singularity occurs at a finite time and position in an unsteady boundary layer evolving under a prescribed pressure distribution. The consequences of its existence are large, particularly for the inviscid flow. It seems possible, however, that previous uncertainties have arisen from inability to calculate accurately unsteady flows with large reversal. For their calculations van Dommelen & Shen made use of a Lagrangian formulation of the two-dimensional unsteady boundary-layer equations and considered a circular cylinder started impulsively from rest. They confirmed the existence of a singularity and the accuracy of their method. It is to be expected that the singularity will also exist in an Eulerian formulation, but many previous attempts, for example, those of Belcher *et al.* (1971) and Telionis & Tsahalis (1974) have failed to reveal it. Useful reviews of the topic have been provided by Riley (1975), Williams (1977), Shen (1978), Telionis (1979) and Cebeci (1982).

With his Eulerian formulation, Cebeci (1979) performed calculations for the same problem. The results extended to $\tau = 2.8$, at which time they were terminated because the shear layers became too thick to be accurately represented by the numerical scheme. Also, a maximum and a minimum developed in the displacement-thickness distribution and tended to cause the solutions to oscillate. Subsequent calculations with an improved transformation allowed solutions up to $\tau = 3.0$ but the non-monotonic variations of the displacement thickness remained (Cebeci 1982). The results were in close agreement with those of van Dommelen & Shen (1982) up to around $\tau = 2.75$.

Consideration of the above results led to a tentative conclusion that the numerical scheme was at fault and that previous Eulerian formulations may have had similar numerical shortcomings. Further calculations were performed to investigate systematically the influence of step lengths in time and x-direction and confirmed that the non-monotonic variation of displacement thickness could be reduced by the use of smaller step lengths but an optimum relationship between Δt and Δx could not be determined and appeared essential. These calculations were performed with a form of Keller's box method modified to include the zigzag formulation of Krause, Hirschel & Bothmann (1968). In common with the often-used Crank–Nicolson method (1947), this scheme is convenient, particularly since the orientation of the numerical mesh is chosen *a priori*. This advantage has a corresponding and potentially dangerous drawback in the presence of large reverse flows since the mesh ratio must be related to the velocity according to the famous Courant– Friedricks–Lewey (CFL) condition (Isaacson & Keller 1966 and Keller 1978) if stability is to be achieved. For a fixed grid chosen *a priori*, this condition may be violated as the flow velocities are determined in ever-increasing computational domains. Thus a natural boundary limiting the domain in which stable computations can be made is also determined *a priori*.

Here we describe a new numerical scheme which is intelligent in the sense that it examines the choice of grid in relation to the magnitude and direction of the local velocity and reaches and implements a decision which ensures that the CFL condition is satisfied. It is applied to the time-dependent equations of the following section and makes use of a form of the characteristic box scheme described in §3. The results for an impulsively started circular cylinder are presented and discussed in §4.

2. Basic equations

We consider incompressible unsteady laminar flow over a circular cylinder started impulsively from rest. The governing boundary-layer equations and their boundary conditions for this flow are well known, see for example Cebeci (1979), and are given by

$$\frac{\partial u}{\partial x}+\frac{\partial v}{\partial y}=0, \tag{1}$$

$$\frac{\partial u}{\partial t}+u\frac{\partial u}{\partial x}+v\frac{\partial u}{\partial y}=u_{\mathrm{e}}\frac{\mathrm{d}u_{\mathrm{e}}}{\mathrm{d}x}+\nu\frac{\partial^2 u}{\partial y^2}, \tag{2}$$

$$y=0,\ u=v=0; \quad y\to\infty,\ u\to u_{\mathrm{e}}(x). \tag{3}$$

To generate the initial conditions for the above equations at $t=0$ and to put them into a more convenient form for solution, we define the similarity variable η and a dimensionless stream function $f(x,\eta,\tau)$ by

$$\eta=\left(\frac{u_0}{\nu L\tau}\right)^{\frac{1}{2}}y, \quad f(\bar{x},\eta,\tau)=\frac{\psi}{(\nu u_0 L\tau)^{\frac{1}{2}}\bar{u}_{\mathrm{e}}}, \tag{4}$$

where ψ is the usual definition of stream function which satisfies (1), u_0 denotes a reference velocity $2\pi u_\infty$, L is a reference length equal to πa with a corresponding to the cylinder radius, τ is a dimensionless time equal to $u_0 t/L$, $\bar{u}_{\mathrm{e}}$ is a dimensionless velocity u_{e}/u_0 and $\bar{x}=x/L$. In terms of these relations, with primes denoting

differentiation with respect to η, (1)–(3) can be written as

$$f''' + \tfrac{1}{2}\eta f'' + \tau \frac{\mathrm{d}\bar{u}_e}{\mathrm{d}\bar{x}} [1 - (f')^2 + ff''] = \tau \left[\frac{\partial f'}{\partial \tau} + \bar{u}_e \left(f' \frac{\partial f'}{\partial \bar{x}} - f'' \frac{\partial f}{\partial \bar{x}} \right) \right], \tag{5}$$

$$\eta = 0, f = f' = 0; \quad \eta = \eta_e, f' = 1. \tag{6}$$

These variables are employed only in the interval during which the boundary layer develops slowly. At higher values of time, the exponential-like growth of the boundary-layer thickness with time near the rear-stagnation-point region is represented in terms of the dimensionless variables Y and F defined by

$$Y = \left(\frac{u_0}{\nu L} \right)^{\frac{1}{2}} y \, \mathrm{e}^{1-\tau}, \quad \psi = (\nu u_0 L)^{\frac{1}{2}} \mathrm{e}^{\tau - 1} \bar{u}_e F(\bar{x}, Y, \tau), \tag{7}$$

and (1)–(3) become

$$F''' + b\eta F'' + b \frac{\mathrm{d}\bar{u}_e}{\mathrm{d}\bar{x}} [1 - (F')^2 + FF''] = b \frac{\partial F'}{\partial \tau} + b\bar{u}_e \left[F' \frac{\partial F'}{\partial \bar{x}} - F'' \frac{\partial F}{\partial \bar{x}} \right] \tag{8}$$

$$Y = 0, F = F' = 0; \quad Y = Y_e, F' = 1. \tag{9}$$

Here $b = \mathrm{e}^{2(\tau - 1)}$ and the primes denote differentiation with respect to Y.

Equations (5) and (8) can also be expressed in the common form:

$$f''' + b_1 \eta f'' + b \frac{\mathrm{d}\bar{u}_e}{\mathrm{d}\bar{x}} [1 - (f')^2 + ff''] = b \frac{\partial f'}{\partial \tau} + b\bar{u}_e \left(f' \frac{\partial f'}{\partial \bar{x}} - f'' \frac{\partial f}{\partial \bar{x}} \right), \tag{10}$$

where, with $f = F$ for $\tau > \tau_*$,

$$b_1 = \begin{cases} \frac{1}{2}, & \tau \leqslant \tau_*, \\ \mathrm{e}^{2(\tau - 1)}, & \tau > \tau_*; \end{cases} \quad b = \begin{cases} \tau, & \tau \leqslant \tau_*, \\ b_1, & \tau > \tau_*. \end{cases}$$

The initial conditions at $t = 0$ can be obtained from (10), which reduces to

$$f''' + \tfrac{1}{2}\eta f'' = 0 \tag{11}$$

and whose solution, subject to (6), is given by

$$f = \eta \operatorname{erf}(\tfrac{1}{2}\eta) + \frac{2}{\sqrt{\pi}} [\exp(-\tfrac{1}{4}\eta^2) - 1]. \tag{12}$$

The initial conditions along the (τ, η)-plane at the forward and rear stagnation points can also be obtained from (10). If the external velocity distribution is represented by

$$\bar{u}_e = \frac{1}{\pi} \sin(\pi \bar{x}), \tag{13}$$

then, at $\bar{x} = 0$ and 1, (10) becomes

$$f''' + b_1 \eta f'' + b\lambda [1 - (f')^2 + ff''] = b \frac{\partial f'}{\partial \tau}, \tag{14}$$

where $\lambda = 1$ for $\bar{x} = 0$ and $\lambda = -1$ for $\bar{x} = 1$.

3. Numerical method

The solution of the time-dependent boundary-layer equations with no flow reversal in u across the layer is routine and can be achieved easily with the Keller (1974) or Crank–Nicolson method (1947). These procedures are described in several references, see for example Bradshaw, Cebeci & Whitelaw (1981). When there is flow reversal, however, the solution of the time-dependent boundary-layer equations is not straightforward and requires special procedures to avoid the numerical instabilities. The zigzag formulation of Krause *et al.* (1968) helps to remedy the difficulties but is not sufficient in all cases, as we shall discuss later. An accurate and physically sound numerical method is the characteristic scheme developed for three-dimensional steady boundary-layer flows by Cebeci & Stewartson (1978, unpublished work) which is based on the solution of governing equations along local streamlines. It examines the finite-difference grid in relation to the magnitude and direction of local velocity and reaches and implements a decision to ensure that the CFL criterion is not violated. A brief description of this method for the problem of the impulsively started cylinder is given below.

We first define a new variable θ as

$$\theta = b\frac{\mathrm{d}\bar{u}_e}{\mathrm{d}\bar{x}}f + b\bar{u}_e\frac{\partial f}{\partial \bar{x}} \tag{15}$$

and write (10) as

$$f''' + b_1\eta f'' + \theta f'' + b\frac{\mathrm{d}\bar{u}_e}{\mathrm{d}\bar{x}}[1-(f')^2] = b\frac{\partial f'}{\partial \tau} + b\bar{u}_e f'\frac{\partial f'}{\partial \bar{x}}. \tag{16}$$

One of the basic ideas of Keller's box method is to write (16) in the form of a first-order system. For this purpose we denote f' by g, let

$$g' = w \tag{17}$$

and write (15) and (16) and their boundary conditions as

$$\theta' = b\frac{\mathrm{d}\bar{u}_e}{\mathrm{d}\bar{x}}g + b\bar{u}_e\frac{\partial g}{\partial \bar{x}}, \tag{18}$$

$$w' + b_1\eta w + \theta w + b\frac{\mathrm{d}\bar{u}_e}{\mathrm{d}\bar{x}}(1-g^2) = b\frac{\partial g}{\partial \tau} + b\bar{u}_e g\frac{\partial g}{\partial \bar{x}}, \tag{19}$$

$$\eta = 0,\ \theta = g = 0; \quad \eta = \eta_e,\ g = 1. \tag{20}$$

The solution of the system given by (17)–(20) by the standard or characteristic box methods depends on how the difference equations are written for (19); the remaining equations are unchanged. In the following paragraphs we first consider (17) and (18) and show how the different equations are written.

Consider the net cube shown in figure 1 and denote the net points by

$$\left.\begin{aligned} &\bar{x}_0 = 0, \quad \bar{x}_i = \bar{x}_{i-1} + r_i \quad (i = 1,2,\ldots,I),\\ &\tau_0 = 0, \quad \tau_n = \tau_{n-1} + k_n \quad (n = 1,2,\ldots,N),\\ &\eta_0 = 0, \quad \eta_j = \eta_{j-1} + h_j \quad (j = 1,2,\ldots,J), \end{aligned}\right\} \tag{21}$$

where $r_i = \Delta\bar{x}_i$, $k_n = \Delta\tau_n$ and $h_j = \Delta\eta_j$.

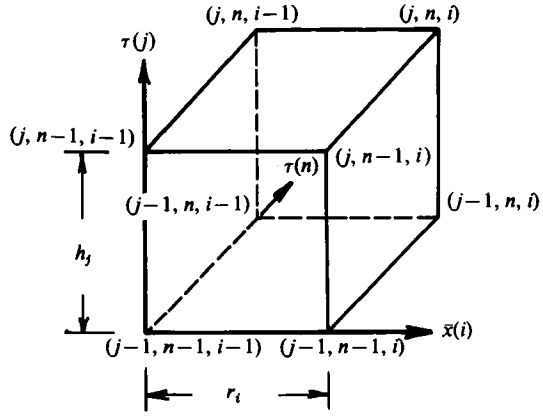

FIGURE 1. Net cube for the difference equations.

The difference approximations that are to represent (17) are obtained by averaging about the midpoint $(\bar{x}_i, \tau_n, \eta_{j-\frac{1}{2}})$,

$$h_j^{-1}(g_j^{i,n} - g_{j-1}^{i,n}) = w_{j-\frac{1}{2}}^{i,n}, \tag{22}$$

where, for example,

$$w_{j-\frac{1}{2}}^{i,n} = \tfrac{1}{2}(w_j^{i,n} + w_{j-1}^{i,n}). \tag{23}$$

The difference approximations to (18) are obtained by centring all quantities except θ at the centre of the cube $(\bar{x}_{i-\frac{1}{2}}, \tau_{n-\frac{1}{2}}, \eta_{j-\frac{1}{2}})$ by taking the values of each variable, say q, at the four corners of the box, that is,

$$q_{j-\frac{1}{2}}^{i-\frac{1}{2},n} = \tfrac{1}{2}(q_{j-\frac{1}{2}}^{i,n} + q_{j-\frac{1}{2}}^{i-1,n}) = \tfrac{1}{4}(q_j^{i,n} + q_j^{i-1,n} + q_{j-1}^{i,n} + q_{j-1}^{i-1,n}). \tag{24a}$$

However, the centring of θ is done by writing it as

$$\theta_{j-\frac{1}{2}}^{i-\frac{1}{2},n-\frac{1}{2}} = \tfrac{1}{2}(\theta_j^{i-\frac{1}{2},n-\frac{1}{2}} + \theta_{j-1}^{i-\frac{1}{2},n-\frac{1}{2}}). \tag{24b}$$

In terms of this notation, the finite-difference approximations to (18) can be written in the following form:

$$h_j^{-1}(\theta_j - \theta_{j-1}) - \left(b\frac{\mathrm{d}\bar{u}_e}{\mathrm{d}\bar{x}}\right)^{i-\frac{1}{2},n-\frac{1}{2}} \bar{g}_{j-\frac{1}{2}} = (b\bar{u}_e)^{i-\frac{1}{2},n-\frac{1}{2}} r_i^{-1}(\bar{g}_i - \bar{g}_{i-1}), \tag{25}$$

where, for example, $\theta_j = \theta_j^{i-\frac{1}{2},n-\frac{1}{2}}$, $\bar{g}_j = \tfrac{1}{2}(g_j^{i-\frac{1}{2},n} + g_j^{i-\frac{1}{2},n-1})$. (26)

The unknown variables in (25) correspond to $g_j^{i,n}$ and $\theta_j^{i-\frac{1}{2},n-\frac{1}{2}}$ so that, when a solution of the system given by (17)–(20) is obtained, g is computed at (i, n, j) and θ at $(i-\frac{1}{2}, n-\frac{1}{2}, j)$. This modified centring procedure is necessary to avoid oscillations due to the use of the continuity equation in the form given by (15) rather than the use of the stream function, which allows continuity and momentum equations to be expressed as a third-order equation.

With the standard box scheme, the difference approximations corresponding to (19) are formulated in the same way as has been described above. With the characteristic box, however, an alternative procedure is followed and is described below. This scheme is based on the solution of the governing equations along the local streamlines defined by

$$\mathrm{d}\tau = \frac{\mathrm{d}\bar{x}}{g\bar{u}_e}. \tag{27}$$

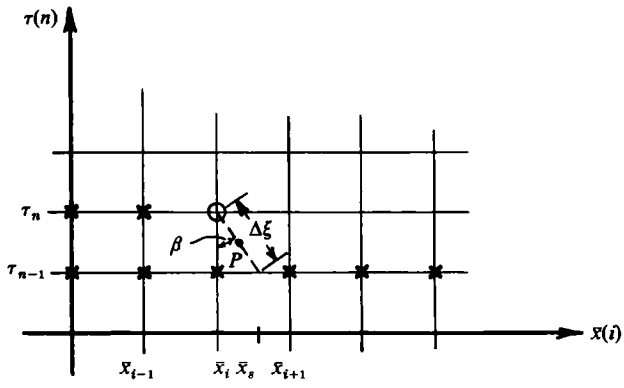

FIGURE 2. Notation for the characteristic box scheme.

If we denote distance in this direction by ξ and the angle that it makes with the τ-axis by β, then (19) can be written as

$$w' + b_1 \eta w + \theta w + b \frac{\mathrm{d}\bar{u}_e}{\mathrm{d}\bar{x}} (1 - g^2) = \lambda \frac{\partial g}{\partial \xi}, \tag{28}$$

where

$$\lambda = b(1 + (\bar{u}_e g)^2)^{\frac{1}{2}}, \tag{29a}$$

$$\beta = \tan^{-1} g. \tag{29b}$$

The finite-difference approximations to (28) are written along the streamline direction (see figure 2). The resulting expressions are lengthy and to illustrate the procedure we consider the model equation

$$w' + \theta w = \lambda \frac{\partial g}{\partial \xi}. \tag{30}$$

With the notation shown in figure 2, the difference approximations to (30) at point P are

$$\tfrac{1}{2}h_j^{-1}(w_j^{i,n} - w_{j-1}^{i,n}) + \tfrac{1}{2}h_j^{-1}(w_j^{s,n-1} - w_{j-1}^{s,n-1}) + \theta^P_{j-\frac{1}{2}} \tfrac{1}{2}(w_{j-\frac{1}{2}}^{i,n} + w_{j-\frac{1}{2}}^{s,n-1}) = \tfrac{1}{2}(\lambda_{j-\frac{1}{2}}^{i,n} + \lambda_{j-\frac{1}{2}}^{s,n-1}) \frac{g_{j-\frac{1}{2}}^{i,n} - g_{j-\frac{1}{2}}^{s,n-1}}{\Delta \xi_j}, \tag{31}$$

where the relation between $\theta^P_{j-\frac{1}{2}}$ and those values of θ centred at $(i-\frac{1}{2}, n-\frac{1}{2})$ and $(i-\frac{3}{2}, n-\frac{1}{2})$ are

$$\theta^P_{j-\frac{1}{2}} = \frac{\theta_{j-\frac{1}{2}}^{i-\frac{3}{2}} - \theta_{j-\frac{1}{2}}^{i-\frac{1}{2}}}{\bar{x}_{i-\frac{3}{2}} - \bar{x}_{i-\frac{1}{2}}} (\bar{x}^P - \bar{x}_{i-\frac{3}{2}}) + \theta_{j-\frac{1}{2}}^{i-\frac{3}{2}}. \tag{32}$$

The boundary conditions follow from (9) and can be written as

$$g_0 = \theta_0 = 0; \quad g_J = 1. \tag{33}$$

The algebraic system given by (22), (25) and (31) together with the boundary conditions given by (33) is nonlinear. Linearization is achieved with Newton's method and the equations are then solved by the block elimination method described, for example, in Bradshaw *et al.* (1981).

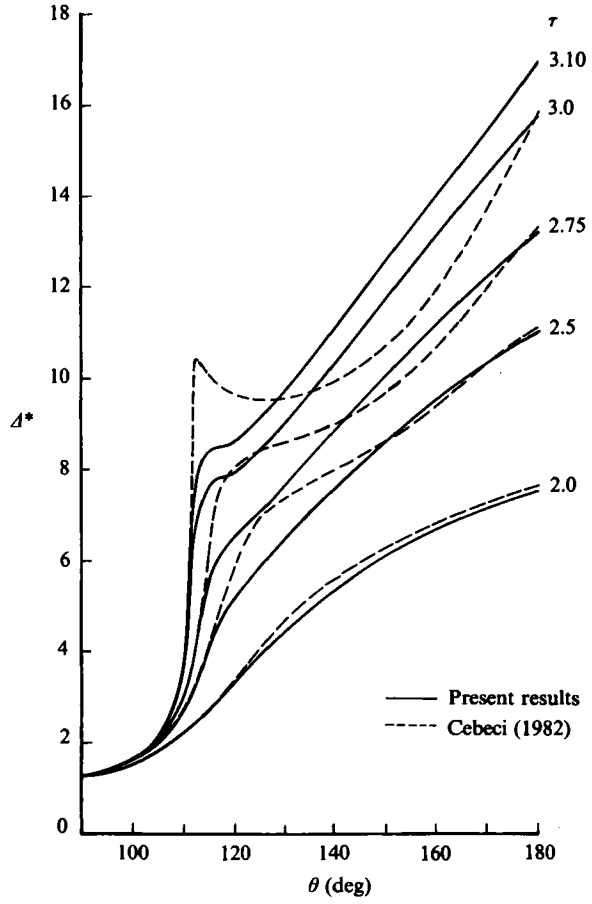

FIGURE 3. Variation of dimensionless displacement thickness.

In the calculations described in the next section, the standard box scheme has been used for all situations when there is no flow reversal. Where a calculation with the standard box reveals a flow reversal ($g_j < 0$) further iterations at that location make use of the characteristic scheme for $g_j < 0$ and the standard box for $g_j > 0$. This switch from one scheme to another continues to allow quadratic convergence and ensures that, provided the step lengths in the τ-and $\bar{x}$-directions are 'properly' selected, the numerical instabilities are avoided. Further details are provided in the next section.

4. Results

It is convenient to present the results which we have obtained using the combination of standard and characteristic box schemes and then to discuss them in relation to previous calculations. Finally, the numerical requirements of the present results are discussed together with the implications of the results for future calculations of more realistic unsteady flows.

Figures 3, 4 and 5 display the variations of dimensionless displacement thickness

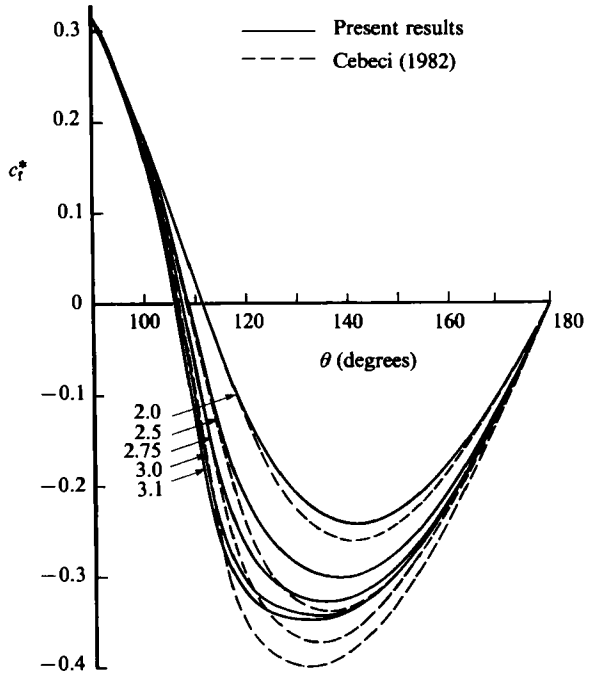

FIGURE 4. Variation of dimensionless local skin-friction coefficient.

Δ^*, local skin-friction coefficient c_f and displacement velocity $\bar{v}_w$, that are defined, with $R_L = u_0 L/\nu$, by

$$\left.\begin{aligned} \Delta^* &= \frac{R_L^{\frac{1}{2}}}{L}\int_0^\delta \left(1-\frac{u}{u_e}\right) \mathrm{d}y, \\ c_f^* &= \frac{2\tau_w}{\rho u_0^2} R_L^{\frac{1}{2}}, \\ \bar{v}_w &= \frac{v_w}{u_0} = \frac{\mathrm{d}}{\mathrm{d}\bar{x}}(\bar{u}_e \Delta^*). \end{aligned}\right\} \tag{34}$$

It is noteworthy that the displacement thickness is close to monotonic with the small maximum and minimum for $\tau = 3.1$ at which the calculations were terminated. The previous results of Cebeci (1982) are also shown in the figure and reveal the maxima which stemmed from the use of a numerical scheme which did not meet the requirements imposed by the CFL condition.

The distributions of local skin-friction coefficients of figure 4 show trends which are similar to those of the previous results but with differences in magnitude consistent with those of figure 3. It should be noted that the results of figures 3 and 4 are identical with those previously obtained up to the value of θ at which the displacement-thickness gradient reaches its maximum and for values of τ less than around 2.75. The differences for large values of θ and τ are associated with the numerical procedure and, in particular, with its ability to satisfy the CFL condition as is discussed later.

The dimensionless displacement velocity $\bar{v}_w$ is shown in figure 5 together with the locus of points corresponding to its maxima which increases with time and decreasing

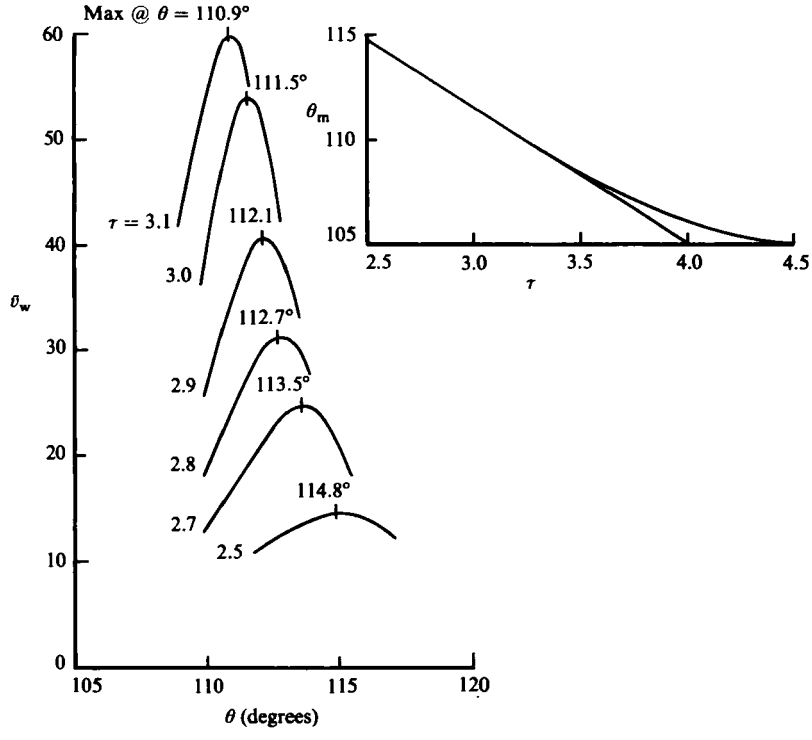

FIGURE 5. Variation of dimensionless displacement velocity. The insert shows the variation of the location of maximum displacement velocity θ_m with circles indicating the computed values, the dashed line the linear extrapolation of θ_m and the solid a line a conjectured variation of θ_m to steady state.

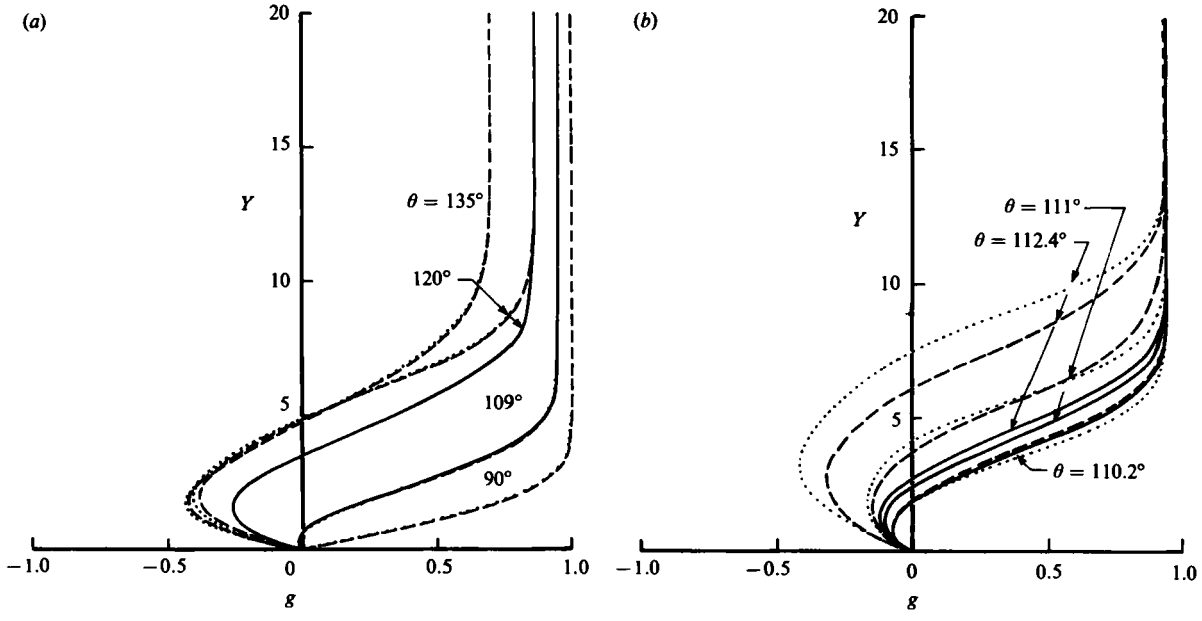

FIGURE 6. Velocity profiles at different times: ——, present method; – – –, Cebeci (1982); . . . ., van Dommelen & Shen (private communication). (*a*) $\tau = 2.75$; (*b*) ——, $\tau = 2.98437$; – – –, 2.9875; . . . ., 3.0.

τ	k_n	$\bar{x}$	r_t
0→1	0.05	0→0.54	0.02
1→1.5	0.02	0.54→0.57	0.01
1.5→2.3	0.01	0.57→0.58	0.0025
2.3→2.73	0.005	0.58→0.60	0.0020
2.73→3.024	0.002	0.60→0.612	0.0015
3.024→3.1	0.001	0.612→0.64	0.0020
		0.64→0.67	0.0025
		0.67→0.72	0.01
		0.72→1.0	0.02

TABLE 1. The distribution of step sizes in τ and $\bar{x}$

angle. At $\tau = 3.0$, the calculated value of θ is 111.5 and corresponds very closely to that determined by van Dommelen & Shen who terminated their calculations at this time. As the peak in the displacement velocity moves upstream with increasing time, the location at which the skin-friction coefficient becomes zero also moves upstream but at a slower rate and towards its steady-state value of 105° (Cebeci & Smith 1974). It may be conjectured that the extrapolation of the peak displacement velocities will asymptote to this steady-state value, but positive confirmation will require excessive computer resources.

Corresponding velocity profiles are presented in figure 6 for $\tau = 2.75$ and 3.0. The general trends are in agreement with those of van Dommelen & Shen and the quantitative values agree closely up to 110°. The discrepancies at larger angles are probably due to the use of inappropriate time steps in the calculations. The previous results of Cebeci (1982) tended to agree with the profiles of van Dommelen & Shen as shown in figure 6(*a*) and are thought to be inaccurate, as is discussed in the following section.

5. Concluding remarks

The previous calculations of Cebeci (1982) were terminated because it proved to be impossible to select the step lengths required to satisfy the CFL condition in the presence of large flow reversal. Other attempts to make use of Eulerian formulations to calculate unsteady flows with large backflow have been plagued by the same difficulty. The need for a measure which would ensure that the CFL condition was satisfied has been met in the present calculations. Here the calculations were performed at a given time and with the step lengths in $\bar{x}$ chosen to have the values shown in table 1. As can be seen, the values of $\Delta\bar{x}$ are very much smaller in the vicinity of singularity. The solutions were iterated at each $\bar{x}$-station until a convergence criterion based on the wall shear parameter f''_w was satisfied, that is

$$|(f''_w)^{\nu+1} - (f''_w)^{\nu}| < \delta_1, \tag{35}$$

where δ_1 is a tolerance parameter which was set equal to 10^{-5} in the calculations.

The keys to the success of the present approach lie in the characteristic box scheme which allows the orientation of the finite-difference mesh to vary across the shear layer and the procedure for the automatic selection of time steps so as to maintain the angle

$$\beta < \tan^{-1} \frac{r_t}{k_n}. \tag{36}$$

The value of k_n was halved until this condition was met. The resulting values of k_n are also shown in table 1 and can be seen to become extremely small at $\tau = 3.0$. The present calculations, which made use of increments in $\bar{x}$, Y and τ of 101, 161 and 435 respectively, could have been extended beyond $\tau = 3.1$ but at considerable expense as witnessed by the small and decreasing values of k_n. The values of k_n and r_i shown in table 1 were subsequently used in conjunction with the zigzag scheme, which had previously failed (Cebeci 1982), to permit calculations for time greater than $\tau > 2.75$. The results were found to be identical to those presented here. The alternative approach of using the zigzag scheme and the relationship given by (36) was not, however, successful. This confirms that it is necessary to allow the flow direction to change across the layer by conditions determined by the local streamlines in the selection of time steps to satisfy the CFL condition, which says that the numerical domain of dependence must include the analytical domain of dependence. This means that the 'mesh triangle' used to advance the solution must contain within it the backward characteristic from the point at which the solution is being computed. In the configuration of figure 2, the CFL condition is assured by (36).

The zigzag scheme does not seem to allow the flexibility to adjust the mesh so that the CFL condition is satisfied. However, if the flow and grid are such that the CFL condition is always satisfied, then the zigzag scheme gives answers that agree very well with the characteristic box scheme. The zigzag scheme using Keller's method remains second-order accurate for flows in which the characteristic slope never changes sign with respect to the grid orientation. Thus the computed results utilizing this method agree well with the standard box method. However, when the characteristic slopes change sign, then the zigzag scheme loses accuracy and is predominantly first-order accurate. Thus with flows with strong backflow, the zigzag scheme is not to be recommended.

It is clear that our new procedure has successfully permitted the calculation of the flow properties for the unsteady flow associated with a cylinder impulsively started from rest. The large reverse-flow regions found with this model problem occur in the more practical application of oscillating airfoils: preliminary work has confirmed that this is so. In particular, the use of the characteristic box scheme together with (36) led to solutions which approached and passed the region of the singularity without numerical difficulty, whereas the zigzag scheme led to solutions which oscillated and broke down in the same manner as experienced with the cylinder.

The above discussion makes it clear that the time steps required to obtain results at the larger values of τ are very small, as was concluded by Ingham (1984). For this reason, the present calculations were terminated at $\tau = 3.1$, which is already larger than that of previous investigators. Figure 5 shows that it is desirable to perform calculations at higher values of τ so as to confirm the conjecture that the only singularity is associated with the steady-state solution. To make a conclusive judgement, calculations should be performed up to $\tau = 4.1$ but, as table 1 suggests, the required time steps are likely to be very small. The time required to obtain results in the range $\tau = 3.024$ to 3.1, which corresponds to 75 time-steps, was 7 hours on a CYBER 175. The computer time likely to be required to reach $\tau = 4.1$ is clearly excessive.

This research was supported under Air Force Office of Scientific Research contract F496720-82-C-0055.

REFERENCES

BELCHER, R. J., BURGGRAF, O. R., COOKE. J. C., ROBINS, A. J. & STEWARTSON, K. 1971 Limitless boundary layers. In *Recent Research on Unsteady Boundary Layers.* In *Proc. Intl Union Theoret. Appl. Mech.* (ed. E. A. Eichelbrenner), pp. 1444–1466.

BRADSHAW, P., CEBECI, T. & WHITELAW. J. H. 1981 *Engineering Calculation Methods for Turbulent Flows.* Academic.

CEBECI, T. 1979 The laminar boundary layer on a circular cylinder started impulsively from rest. *J. Comp. Phys.* **31**, 153–172.

CEBECI, T. 1982 Unsteady separation. In *Numerical and Physical Aspects of Aerodynamic Flows* (ed. T. Cebeci), pp. 265–277. Springer.

CEBECI, T. & SMITH, A. M. O. 1974 *Analysis of Turbulent Boundary Layers.* Academic.

CRANK, J. & NICOLSON, P. 1947 A practical method for numerical evaluation of solutions of partial-differential equations of the heat-conduction type. *Proc. Camb. Phil. Soc.* **43**, 50–67.

INGHAM, D. B. 1984 Unsteady separation. *J. Comp. Phys.* **53**, 90–99.

ISAACSON, E. & KELLER, H. B. 1966 *Analysis of Numerical Methods.* Wiley.

KELLER, H. B. 1974 Accurate difference methods for two-point boundary-value problems. *SIAM J. Numer. Anal.* **11**, 305–320.

KELLER, H. B. 1978 Numerical methods in boundary-layer theory. *Ann Rev. Fluid Mech.* **10**, 417–433.

KRAUSE, E., HIRSCHEL, E. H. & BOTHMANN, TH. 1968 Die numerische Integration der Bewegungsgleichungen dreidimensionaler laminarer kompressibler Grenzschichten, Bd 3, *Fachtagung Aerodynamik, Berlin*; D-LR-Fachlichreihe, 1–49.

RILEY, N. 1975 Unsteady laminar boundary layers. *SIAM Rev.* **17**, 274–297.

SEARS, W. R. & TELIONIS, D. P. 1975 Boundary-layer separation in unsteady flow. *SIAM J. Appl. Maths* **28**, 215–235.

SHEN, S. F. 1978 Unsteady separation according to the boundary-layer equations. *Adv. Appl. Mech.* **18**, 177–200.

TELIONIS, D. P. 1979 Review – Unsteady boundary layers, separated and attached. *Trans. ASME* I: *J. Fluids Engng* **101**, 29–43.

TELIONIS, D. P. & TSAHALIS, D. T. 1974 Unsteady laminar separation over impulsively moved cylinders. *Acta Astron.* **1**, 1487–1505.

VAN DOMMELEN, L. L. & SHEN, S. F. 1981 The spontaneous generation of the singularity in a separating laminar boundary layer. *J. Comp. Phys.* **38**, 125–140.

VAN DOMMELEN, L. L. & SHEN, S. F. 1982 The genesis of separation. In *Numerical and Physical Aspects of Aerodynamic Flows* (ed. T. Cebeci), pp. 293–311. Springer.

WILLIAMS, J. C. 1977 Incompressible boundary-layer separation. *Ann. Rev. Fluid Mech.* **9**, 113–144.